ANALYSIS OF NON-ORIENTED ELECTRICAL STEEL CORES IN ELECTRICAL MACHINES

Laurentiu DUMITRU[1], Gheorghe PALTANEA[1],
Veronica MANESCU (PALTANEA)[1], Horia GAVRILA[1]

Permanent magnet synchronous motors are a highly reliable electrical machine with an increase energy efficiency due to the use of performant magnetic cores. In this paper is numerically analyzed a configuration of a synchronous motor that uses two types of non-oriented electrical steel as magnetic core laminations. The first alloy is M300-35A that is a low energy loss material, with the smallest thickness possible, and the other one is a more common material M700-50A, with increased thickness and energy losses, used in the manufacture process of high efficiency motors. The electromagnetic field problem is computed numerically using a finite element method software, driven by a MATLAB code that perform the rotation of the rotor at a step of 1º, records the data of the magnetic flux density matrix and torque. Using the Steinmetz method, the power losses in rotor and stator are calculated at a speed range from 100 to 8000 rot/min.

Keywords: permanent magnet synchronous motor, non-oriented electrical steel, power losses, Steinmetz coefficients, finite element method

1. Introduction

Electrical motors are the most important equipment in the motion generation mechanisms in industry and in household devices. When an electrical machine is designed, this operation should be made, by taking into account the existing standards, the availability of the magnetic materials on the market, their quality and costs, and the cutting procedure of the magnetic cores [1]. Important parameters of the electrical machines are the power range, the electrical machine size and its application. The goal of the electrical motor design is the analyze of the machine energy efficiency and taking it as a start point, it should be chosen a given geometry (windings, frame and stator or rotor cores) and adequate quality materials for the magnetic core manufacture, in order to obtain low values of the electrical, mechanical and magnetic losses [2]. The final product is usually difficult to manufacture in some particular cases, because of its complexity, constraints of the fabrication processes, time and cost resource limits [3].

[1] Electrical Engineering Dept., University POLITEHNICA of Bucharest, Romania, corresponding author: laurdumitru@yahoo.com

Nowadays the man intervention in the manufacturing process of the electrical machines is very important, because an experienced engineer chooses the high efficiency materials, from which the motors' magnetic cores are made. In order to begin the electrical machine project, the steady state parameters, electrical power, speed domain, electrical currents, motor efficiency, power factor (for AC electrical machines), and dynamic performances should be known [4, 5]. The Computer – Aided Engineering (CAE) is firstly used for the working faults' identification, then for the analysis, computations and simulations of the electrical motors. The libraries and databases of the CAE software are very important, especially the material library, because every material has to be defined, by respecting the producer specifications, and to include the electrical, magnetic, thermic and mechanical parameter values. Another limitation in the electrical motor design is the fact that complex 2D or 3D simulations require powerful computers, because of the geometrical model complexity.

The three phased power supplied induction motor (IM) is the most used electrical machine in the industry. The asynchronous motor consists usually of a stator and a rotor. The squirrel-cage motors have axial rotor bars, made by aluminum or copper, with two short-circuited end-rings. The stator windings are supplied trough a symmetrical three phased currents [6, 7]. It is generated a rotating magnetic field that has as a result, an induced current in the rotor bars, with a frequency different from the stator currents. These rotor currents induce another magnetic field and the electrical machine torque appears only if the rotor moves slowly than the stator [8].

The energy conservation worldwide trend leads to the need of increasing the energy efficiency of the electrical machines. The permanent magnet (PM) are intensively used, because of their high-energy product, and brushless PM electrical machines have been adopted as a very popular technology in many applications as industrial servomotors for electric/hybrid electric vehicles and more-electric aircrafts [9, 10]. A PM servomotor is a synchronous machine that has a feedback for velocity, commutation and position information. The rotor size is smaller than that of a similar power induction motor, fact that will have an effect on the motor inertia. Exactly as in the case of IM, the stator is powered by a symmetrical three-phased current system and it generates a rotating magnetic field. The PM polar faces are placed on the rotor in alternating positions that combined the stator rotating magnetic field determines the rotation movement of rotor core at a synchronous frequency, equal to that of stator rotating field [11].

The performances of the IMs and PM servomotors overlap, but these types of electrical machines are not considered a replacement of each other. Today, due to the technological advancements of the IMs' manufacture they can have dynamic performances, comparable to those of PM servomotors. Both types of

motors are able to have high torque, speed and good thermal effects, but when the size of the motor is important PM servomotors are chosen.

In the paper it is studied an original PM electrical motor geometry with magnetic core made of two non-oriented electrical steels. One type of steel is a standard grade, used in the IE3 premium efficiency configuration and the other one, a thinner high-quality grade is used in the IE4 super premium efficiency machines. An electromagnetic field problem, which modeled the proposed geometrical configuration of the motor, was implemented in a finite element method (FEMM 4.2) software. A MATLAB program was linked to the electromagnetic problem and it performs the rotation of the rotor at a step of 1º, records the data of the magnetic flux density matrix and torque. Based on Steinmetz method the model coefficients for each analyzed material are determined, and the power losses in rotor and stator are calculated at a speed range from 100 to 8000 rot/min.

2. Numerical model

To compute the electromagnetic field distribution, it was used a finite element model program (FEMM 4.2), based on triangular elements discretization mesh [12].

Fig. 1. Motor design model.

The analyzed geometrical structure of the electrical motor is presented in Fig.1. The axial length of the magnets, rotor core and stator laminations are 0.06 m. The stator has 12 slots that present a three phase windings' wiring diagram, each coil having 43 turns wrapped around a stator tooth (Fig. 2). The copper wire used for the coils is AWG 25 and a current of 2 A flows through it.

The outer diameter of the stator is equal to OD_s = 111 mm. On the rotor (OD_r = 64 mm) are placed 10 NdFeB (N40SH), parallel-magnetized permanent magnets, in an antiparallel arrangement. The electrical conductivity of the N40SH is 0.694 MS/m and the coercive magnetic field strength is 980 kA/m. The catalog data of the demagnetization curves is presented in Fig. 3. In the numerical simulation we have used the data for 100 °C.

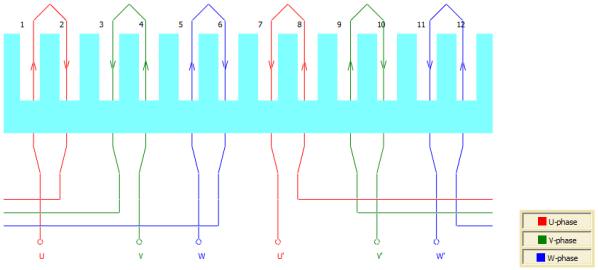

Fig. 2. Electrical connection diagram for the stator windings.

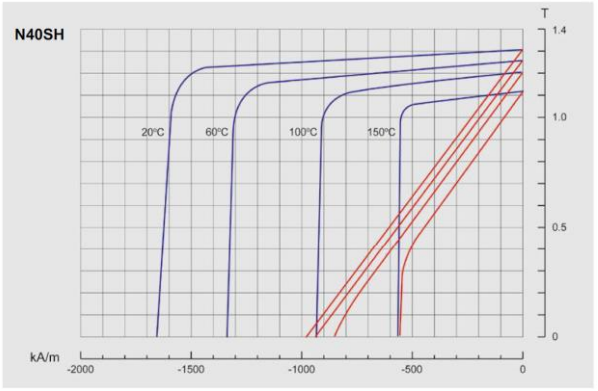

Fig. 3. Demagnetization curves for NdFeB (N40SH) permanent magnets [13].

Two non-oriented electrical steels were considered for the stator and rotor cores, M300-35A and M700-50A. The physical properties of the alloys are presented in Table 1. The normal magnetization curves that were used in the non-linear calculation in the FEMM software are shown in Fig. 4.

Table 1

Physical properties of the electrical steel magnetic core

Material	Thickness [mm]	Density [kg/m^3]	Resistivity [μΩm]	Relative permeability
M300-35A	0.35	7.65	0.5	830
M700-50A	0.5	7.8	0.25	1730

The prediction of the core losses in the modeled electrical machine was based on the experimentally determined variation of the total power losses as function of magnetic polarization (Fig. 5).

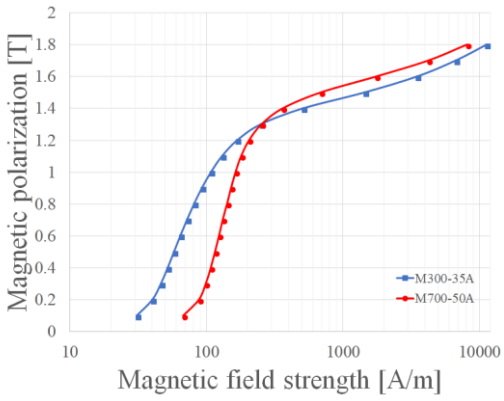

Fig. 4. Normal magnetization curve measured at 50 Hz in the case of the two studied materials

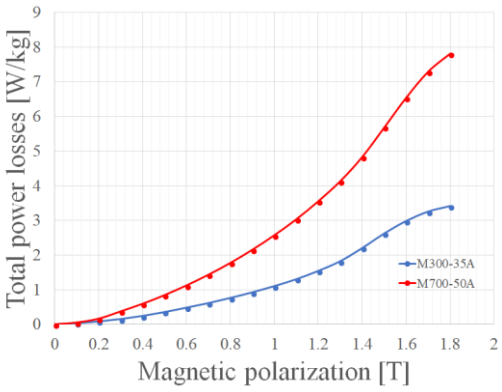

Fig. 5. Total power losses as function of magnetic polarization at 50Hz for the two electrical steels.

Previous studies [14, 15] use specific models of the magnetic core loss mechanism taking into account the separation of power losses into hysteresis, classical and excess components, that were incorporated into *J-H* relationship. After that, the resulted magnetization curve was used in the time-transient model of the motor to express the voltages and currents.

In this paper, the Steinmetz formulation (eq. 1) of the total power losses was applied considering two components: the hysteresis one, which varies linearly with the frequency, and the classical part that has a variation directly proportional with the square of frequency:

$$P_{tot} = P_h + P_{cl} = 2\pi f \cdot C_h J^2 + 4\pi^2 f^2 C_{cl} J^2, \tag{1}$$

where C_h and C_{cl} are the hysteresis and dynamic loss coefficient, respectively [16, 17]. These two parameters are determined through fitting procedures on the experimentally determined curves from Fig. 5 [18, 19]. For a given frequency f

and magnetic polarization J, the total power losses in the magnetic material can be computed. The fitted parameters for the two used materials are presented in Table 2.

Table 2

Parameters used to compute de total power loss variation $P_{tot}(J)$

Material	C_h [W/m^{3}T^{2}Hz]	C_{cl} [W/m^{3}T^{2}Hz^2]
M300-35A	143	0.530
M700-50A	68	0.044

The numerical simulation was made by considering the synchronous motor equations, used to compute the currents' values in the stator windings as a function of the rotor position, as if it performed a complete rotation. At each step, a magneto-static problem was computed, and it was recorded the position of each triangular elements that are part of the rotor structure and their magnetic properties. A MATLAB program was developed, in order to perform a series of finite element runs, which increments the rotor position, computes the stator currents for every step and saves the magnetic properties from the motor structure.

The entire structure was discretized, using 39759 triangular elements (Fig. 6). Over each element, the solution is approximated by a linear interpolation of the values of the magnetic potential at the tip vertices of the triangle. The linear algebra problem is determined, minimizing an error between the exact differential equation of the electromagnetic field and the approximate differential equation. On the outer and inner contours of the geometry, null Dirichlet (fixed) boundary conditions were set [12].

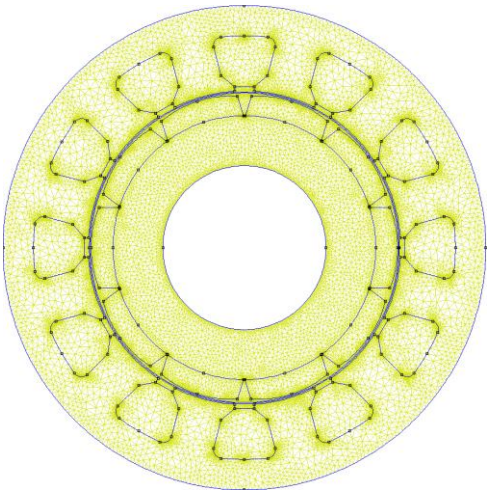

Fig. 6. The triangular discretization mesh used in order to compute the electromagnetic field in the electrical motor.

3. Results and discussion

In Fig. 7 is presented the magnetic flux density color map that is generated by the rotor magnets, when the currents, which power the stator, are equal to zero.

It can be observed that permanent magnets' magnetic flux density has a maximum value of approximately 1.6 T that is observed in the stator teeth.

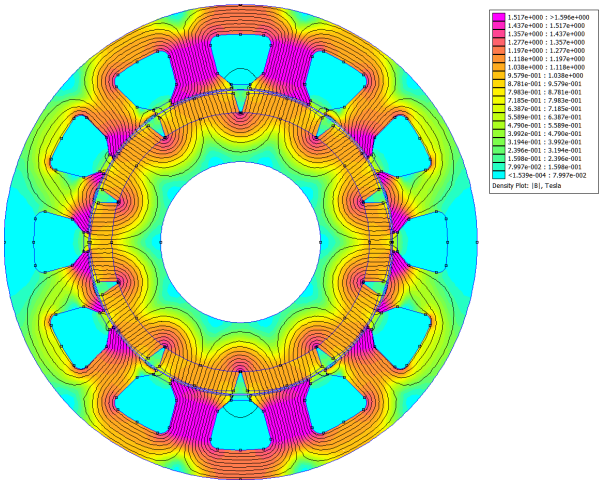

Fig. 7. Color map distribution of the magnetic flux density and flux lines contours generated by the rotor magnets in the case of M300-35A electrical steel laminations.

As computation theory it was applied the Maxwell stress tensor, which takes into account only the local magnetic flux that flows along a line or a given contour. The electromagnetic forces could be computed as it follows:

$$\mathbf{F}=\iint\left[\frac{1}{\mu_0}\mathbf{B}\left(\mathbf{B}\cdot\mathbf{n}\right)-\frac{1}{2\mu_0}\mathbf{B}^2\mathbf{n}\right]dA, \tag{2}$$

with two components $F_n=\frac{L_i}{2\mu_0}\int\left(B_n^2-B_t^2\right)dl$ the normal and $F_t=\frac{L_i}{\mu_0}\int\left(B_nB_t\right)dl$ the tangential part. The quantities **n**, *dA*, *dl*, L_i, B_n and B_t are the normal to the integral surface, surface element, elementary arc length, stack length, normal and tangential components of the magnetic flux density **B**. The torque could be computed, by starting from its definition $\mathbf{T}=\mathbf{r}\times\mathbf{F}$ according to eq. 3:

$$T=\frac{L_i}{2\mu_0}\int rB_nB_tdl, \tag{3}$$

where r is the radius of the circumference traced in the middle of the air gap. The Maxwell stress tensor integration uses a precise solution in the air gap, based on a fine discretization of the model, because the magnetic flux density is not continuous at the nodes and across boundaries of the discretization triangles [20, 21].

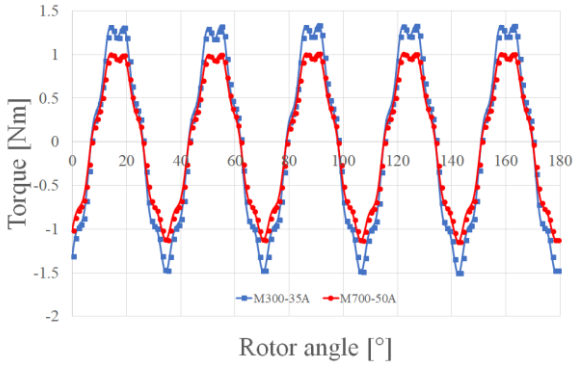

Fig. 8. Peak torque as a function of rotor angle.

In Fig. 8 is presented the peak torque of the electrical machine as a function of the rotor angle, in the case of two electrical steels. Cogging torque is defined as an oscillation, which is due to the energy modification in an electrical motor, when the currents in stator are equal to zero and it is usually associated with the shift of the rotor magnetic field to align with the stator poles. The sum of the cogging torque and torque ripple determines variations of the torque that creates vibrations and noise, during motor working program [22, 23].

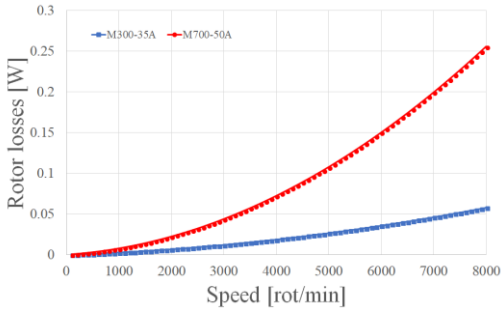

Fig. 9. Rotor power losses versus speed.

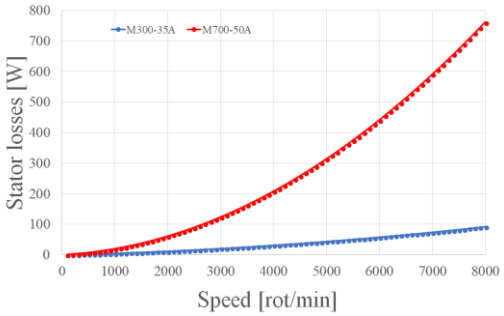

Fig. 10. Stator power losses versus speed.

In Fig. 9 and Fig. 10 are presented the variations of the rotor and stator power losses versus the speed of the electrical motor. For the computation of the power losses in the magnetic core, the magnetic flux density from every triangular element, which is located in stator and rotor, respectively, is stored for every rotor position. The resulted matrix of fluxes is used to determine the power losses as a

function of the rotor mechanical speed, by considering it as the frequency in eq. 1. It can be observed that the high-quality steel and the reduced thickness of the lamination determine lower power losses in the machine.

4. Conclusions

A model of an electrical machine with permanent magnets was developed in FEMM software that is a useful and free program, used for electromagnetic field problem computations. The finite elements' technique can usually analyze permanent magnets' circuits and motors. A MATLAB program was done, in order to compute the torque and the power losses in stator and rotor of the motor. Two electrical steels were considered for the magnetic circuit of the rotor and stator, and it can be concluded that the developed programs and simulations are valid for both materials.

Acknowledgements

The work of Gheorghe PALTANEA has been funded by University Politehnica of Bucharest, through "Excellence Research Grants" Program, UPB-GEX 2017. Identifier: UPB-GEX2017, Ctr. No. 02/25.09.2017 (ANIZ-GO). The work of Veronica MANESCU (PALTANEA) has been funded by University Politehnica of Bucharest, through "Excellence Research Grants" Program, UPB-GEX 2017. Identifier: UPB-GEX2017, Ctr. No. 04/25.09.2017 (OPTIM-IE4). The work of Horia GAVRILA was supported by a grant of the Romanian National Authority for Scientific Research and Innovation, CNCS/CCCDI – UEFISCDI, Project Number 10PTE/2016, within PNCDI III "Brushless servo-motors series utilizing soft magnetic composite materials".

R E F E R E N C E S

[1]. *S. Orlova, A. Rassolkin, A. Kallaste, T. Vaimann, and A. Belahcen*, "Lifecycle analysis of different motors from standpoint of environmental impact", Latv. J. Phys. Tech. Sci., **vol. 53**, no. 6, 2016, pp. 37-46.

[2]. *G. Lei, J. Zhu, and Y. Guo*, Multidisciplinary design optimization methods for electrical machines and drive system, Springer-Verlag, Berlin, 2016.

[3]. *V. Manescu (Paltânea), G. Paltanea, H. Gavrila, G. Scutaru, I. Peter*, "High efficiency electrical motors state of the art and challenges", Rev. Roum. Sci. Techn. - Série Électrotechnique et Énergétique, **vol. 62**, no. 1, 2017, pp. 14-18.

[4]. *K. Daukaev, A. Rassolkin, A. Kallaste, T. Vaimann, and A. Belahcen*, "A review of electrical machine design processes from the standpoint of software selection", IEEE 58th Int. Sci. Conf. on Power and Electrical Engineering of Riga Technical University, 2017.

[5]. *D. Kowal, P. Sergeant, L. Dupre, and A. Van den Bossche*, "Comparison of nonoriented and grain-oriented material in an axial flux permanent-magnet machine", IEEE Trans. Magn., **vol. 46**, no. 2, 2010, pp. 279–285.

[6]. *S. Lopez, B. Cassoret, J.-F. Brudny, L. Lefebvre, and J. Vincent*, "Grain oriented steel assembly characterization for the development of high efficiency AC rotating electrical machines", IEEE Trans. Magn., **vol. 45**, no. 10, 2009, pp. 4161–4164.
[7]. *B. Cassoret, S. Lopez, J.-F. Brudny, and T. Belgrand*, "Non-segmented grain oriented steel in induction machines", Progress Electromagnetics Res. C, **vol. 47**, 2014, pp. 1–10.
[8]. *H. Gavrila, V. Manescu (Paltanea), G. Paltanea, G. Scutaru, I. Peter*, "New Trends in Energy Efficient Electrical Machines", Procedia Engineering, **vol. 181**, 2017, pp. 568-574.
[9]. *R. Kolano, K. Krykowski, A. Kolano-Burian, M. Polak, J. Szynowski, and P. Zackiewicz*, "Amorphous soft magnetic materials for the stator of a novel high-speed PMBLDC motor", IEEE Trans. Magn., **vol. 49**, no. 4, 2013, pp. 1367–1371.
[10]. *Z. Wang, Y. Enomoto, M. Ito, R. Masaki, S. Morinaga, H. Itabashi, and S. Tanigawa*, "Development of a permanent magnet motor utilizing amorphous wound cores", IEEE Trans. Magn., **vol. 46**, no. 2, 2010, pp. 570-573.
[11]. *A. Schoppa and P. Delarbre*, "Soft magnetic powder composites and potential applications in modern electric machines and devices", IEEE Trans. Magn., **vol. 50**, no. 4, 2014, pp. 1-4.
[12]. *** FEMM 4.2, User's Manual, 2018.
[13]. *** Sintered neodymium iron boron (NdFeB) magnets, Eclipse Magnetics Ltd., Sheffield, UK.
[14]. *E. Dlala*, "Comparison of models for estimating magnetic core losses in electrical machines using the finite-element method", IEEE Trans. Magn., **vol. 45**, no. 2, 2009, pp. 716-725.
[15]. *H. Trabelsi, A. Mansouri, and M. Gmiden*, "On the no-load iron losses calculations of a SMPM using VPM and transient finite element analysis", International Journal of Sciences and Techniques of Automatic Control & Computer Engineering, **vol. 2**, no. 1, 2008, pp. 470-483.
[16]. *L. Petrescu, V. Ionita, E. Cazacu, and C. Petrescu*, "Steinmetz' parameters fitting procedure for the power losses estimation in soft magnetic materials", 2017 International Conference on Optimization of Electrical and Electronic Equipment (OPTIM) & 2017 Intl Aegean Conference on Electrical Machines and Power Electronics (ACEMP), May 2017, pp. 208-213.
[17]. *J. Reinert, A. Brockmeyer and R.W.A.A. de Doncker*, "Calculation of losses in ferro- and ferrimagnetic materials based on the modified Steinmetz equation", IEEE Trans. Ind. App., **vol. 37**, no. 4, 2001, pp. 1055-1061.
[18]. *D.C. Meeker*, "An improved continuum skin and proximity effect model for hexagonally packed wires", Journal of Computational and Applied Mathematics, **vol. 236**, no. 18, 2012, pp. 4635-4644.
[19]. *V. Manescu (Paltanea), G. Paltanea, and H. Gavrila,* "Non-oriented silicon iron alloys – state of the art and challenges", Rev. Roum. Sci. Techn. – Électrotechn. et Énerg., **vol. 59**, no. 4, 2014, pp. 371-380.
[20]. *J.A. Güemes, A.M. Iraolagoitia, J.I. del Hoyo, and P. Fernández*, "Torque analysis in permanent-magnet synchronous motors: A comparative study", IEEE Trans. Energy Convers., **vol. 26**, 2011, pp. 55-63.
[21]. *R. Islam, I. Husain, A. Fardoun, and K. McLaughlin*, "Permanent-magnet synchronous motor magnet designs with skewing for torque ripple and cogging torque reduction", IEEE Trans. Ind. Appl., **vol. 45**, 2009, pp. 152-160.
[22]. *Y. Wang, M.J. Jin, W.Z. Fei, and J.X. Shen*, "Cogging torque reduction in permanent magnet flux-switching machines by rotor teeth axial pairing", IET Electric Power Appl., **vol. 4**, 2010, pp. 500-506.
[23]. *D. Wang, X. Wang, D. Qiao, Y. Pei, S.Y. Jung*, "Reducing cogging torque in surface-mounted permanent-magnet motors by nonuniformly distributed teeth method", IEEE Trans. Magn., **vol. 47**, 2011, pp. 2231-2239.